AGU PUBLICATIONS

Geophysical Research Letters

RESEARCH LETTER
10.1002/2016GL070017

Key Points:
- Simple statistical method to quantify the occurrence of compound precipitation and wind extremes in gridded data sets
- Highest numbers of compound extremes in coastal regions and areas with frequent tropical cyclones
- Orographic modulation of winds and orographic drying of air masses result in strong regional variations in the number of compound extremes

Supporting Information:
- Supporting Information S1

Correspondence to:
O. Martius,
Olivia.martius@giub.unibe.ch

Citation:
Martius, O., S. Pfahl, and C. Chevalier (2016), A global quantification of compound precipitation and wind extremes, *Geophys. Res. Lett.*, *43*, 7709–7717, doi:10.1002/2016GL070017.

Received 27 APR 2016
Accepted 6 JUL 2016
Accepted article online 9 JUL 2016
Published online 25 JUL 2016

A global quantification of compound precipitation and wind extremes

Olivia Martius[1], Stephan Pfahl[2], and Clément Chevalier[3]

[1]Oeschger Centre for Climate Change Research, Institute of Geography, Mobiliar Lab for Natural Risks, University of Bern, Bern, Switzerland, [2]Institute for Atmospheric and Climate Science, ETH Zurich, Zürich, Switzerland, [3]Institut de Statistique, Université de Neuchâtel, Neuchâtel, Switzerland

Abstract The concomitant occurrence of extreme precipitation and winds can have severe impacts. Here this concomitant occurrence is quantified globally using ERA-Interim reanalysis data. A logistic regression model is used to determine significant changes in the odds of precipitation extremes given a wind extreme that occurs on the same day, the day before, or the day after. High percentages of cooccurring wind and precipitation extremes are found in coastal regions and in areas with frequent tropical cyclones, with maxima of more than 50% of concomitant events. Strong regional-scale variations in this percentage are related to the interaction of weather systems with topography resulting in Föhn winds, gap winds, and orographic drying and the structure and tracks of extratropical and tropical cyclones. The percentage of concomitant events increases substantially if spatial shifts by one grid point are taken into account. Such spatially shifted but cooccurring events are important in insurance applications.

1. Introduction

So-called compound extremes, for example, extreme events with a joint occurrence of different types of natural hazards, can have very severe impacts [*Seneviratne et al.*, 2012]. Examples for such concurrent extremes with severe impacts that potentiate each other are as follows: the simultaneous occurrence of storm surges and high river discharges due to precipitation in coastal areas [e.g., *Kew et al.*, 2013] resulting in coastal floods, or the joint effects of heat waves and drought conditions on wild fires [e.g., *Witte et al.*, 2011].

The focus of this study is the concurrent occurrence of wind and precipitation extremes. This combination of extremes also results in significant impacts. For example, if strong winds destroy the roofs of buildings, the concomitant heavy rain causes substantially more damage. Another impact example is the hindered access to affected areas for rescue personnel as a consequence of blocked roads, e.g., by fallen trees or intense snowfall in winter. Further on, trees are more susceptible to wind damage if the soils are very wet. In addition, concomitant wind and precipitation extremes are of great interest for insurance companies, as the interdependence of extremes and their impacts needs to be included in insurance loss models.

Compound extremes can occur by chance and be causally unrelated, or they can be triggered by the same underlying process or weather system [*Seneviratne et al.*, 2012]. Simultaneous wind and precipitation extremes are often related. In the midlatitudes and the subtropics, for example, they can be associated with strong extratropical cyclones [e.g., *Fink et al.*, 2009; *Liberato*, 2014; *Raveh-Rubin and Wernli*, 2015]. In the tropics and subtropics, simultaneous wind and precipitation extremes can be caused by tropical cyclones [*Federal Emergency Management Agency*, 2013; *Rodgers et al.*, 1994].

Several case studies discussing concomitant wind and precipitation extremes exist [e.g., *Fink et al.*, 2009; *Liberato*, 2014; *Raveh-Rubin and Wernli*, 2015]; however, a systematic global quantification of their concomitant occurrence and an estimate of the statistical significance is so far missing and is the focus of this study.

The term concomitant is not unequivocally defined and can refer to different spatial and temporal scales. The relevant spatial scale depends on the impacts. For the impacts described in the first paragraph, the extremes must happen at the same location. Extremes triggered by the same weather system but happening in slightly different locations are highly relevant for insurance loss modeling. Here we use a set of very simple definitions, namely, that (i) wind and precipitation extremes must occur at the same grid point of the ERA-Interim reanalysis data set on the same day, the day before, or the day after; or (ii) they occur on the same day but may be shifted by one grid point.

This allows describing and quantifying the joint occurrence of extremes globally at a relatively coarse resolution. More specifically, the aims of this study are to quantify the occurrence of simultaneous daily precipitation and wind extremes and to discuss the link to the meteorological phenomena responsible for the joint occurrence

2. Data

Extreme events are identified in the ERA-Interim reanalysis data set [*Dee et al*., 2011] for the period January 1979 to December 2012. The data are available with a 6-hourly resolution and interpolated to a 1 by 1° grid mesh in the horizontal. Extremes are defined per grid point as exceedances of the grid point seasonal 98th percentile of the daily accumulated precipitation and the daily maximum near-surface (10 m) wind gusts.

The precipitation in the ERA-Interim data set stems from short-term forecasts and is not constrained by direct precipitation observations. Here we are interested in the time and location of extreme event occurrence rather than in absolute precipitation values. *Pfahl and Wernli* [2012] provide a discussion of the potential and the limitations of the ERA-Interim precipitation data for exactly this type of analysis. They show that the temporal agreement between the occurrence of precipitation extremes in ERA-Interim and a satellite-based precipitation data set is high in the extratropics (mostly above 80%) and quite low in some tropical areas (20 to 30%).

3. Definition of Extremes and Cooccurrence

The choice of the 98th percentile threshold is based on the following considerations. Percentile-based extremes are called "moderate" extremes and frequently used in the analysis of climate extremes [e.g., *Zhang et al*., 2011] because they provide sufficiently large sample sizes for robust statistical assessments. While events in the far tail of the distribution are expected to cause the severest societal and environmental damage [*Zhang et al*., 2011], these moderate extremes are also impact relevant.

Klawa and Ulbrich [2003] show that the local 98th wind percentile is a damage-relevant wind threshold. The choice of an impact-relevant threshold for precipitation is more complex because the impacts are more diverse encompassing floods, surface runoff, and landslides. *Guzzetti et al*. [2008] provide an overview of critical rainfall thresholds for the triggering of shallow landslides and debris flows. These thresholds depend on the duration of the event and the local precipitation climatology. For 24 h precipitation events threshold values correspond to the 98th percentile in some areas. *Froidevaux et al*. [2015] show for Swiss catchments that more than 20% of all flood events with a 5 year return period (RP) are preceded by 2 day sums between the 95th and the 99th percentile (more than 40% if floods with a 1 year RP are considered).

Extracting the local seasonal 98th percentile of the wind and precipitation data results in two 34 year binary time series for each grid point, indicating the presence or absence of extremes. The four seasons are December, January, February (DJF); March, April, May (MAM); June, July, August (JJA); and September, October, November (SON). The values of the wind and precipitation percentiles vary substantially with the season and are shown in Figures S1 and S2 of the supporting information for JJA, DJF, and the entire year. In the extratropics the 98th percentiles of both wind and precipitation are generally largest in the winter season and even exceed the yearly 98th percentiles in some areas. There are some areas where precipitation percentiles are largest in summer, e.g., in eastern Europe and Russia. We also tested yearly percentiles instead of seasonal percentiles. The results for individual seasons are qualitatively very similar; however, the nonsignificant areas increase in the seasons with fewer extremes (Figure S3).

Here the cooccurrence of wind and precipitation extremes is defined in two ways. (i) Cooccurring extremes are defined as events occurring at the same grid point and on the same day or are shifted in time by 1 day. This temporal relaxation takes events into account during which it rains before midnight and extreme winds occur after midnight (or vice versa), but both extremes are associated with the same weather system. These events are highly relevant for the severity of local impacts as described in section 1. (ii) Cooccurring extremes are defined as events occurring on the same day but are shifted in space by one grid point. The motivation for this approach is that precipitation and wind extremes associated with the same cyclone can occur at different locations [e.g., *Bengtsson et al*., 2009; *Pfahl*, 2014; *Raveh-Rubin and Wernli*, 2015].

4. Statistical Approach

We use two approaches to quantify the cooccurrence of the extremes. The first, very simple approach consists of counting the number of cooccurring events. The second, statistically more rigorous approach uses logistic regression to quantify the odds of having a precipitation extreme at a specific grid point given a wind extreme that occurs:

$$\text{Logit}(p(t)) = \beta_0 + \beta_1 \ \text{wind}(t) \tag{1}$$

Where wind(t) is a binary sequence indicating for each time step if a wind extreme occurred at this specific grid point on the same day, the day before, or the day after.

$$\text{Logit}(p(t)) = \log(p(t)/(1-p(t)) \tag{2}$$

Where $p(t) = P\ (\text{prec}(t) = 1 \mid \text{wind}(t))$ is the probability of observing an extreme precipitation event at time t given the wind observations, and $p/(1-p)$ are the odds.

Hereafter, the odds ratios at every grid point, i.e., $\exp(\beta_1)$ (equation (1)) are discussed and shown in the figures. Results are highlighted that are statistically significant at the 95% significance level. The odds ratio $\exp(\beta_1)$ can be interpreted as a multiplicative factor that increases (or decreases, if below 1) the odds of observing a precipitation extreme at a specific grid point, given that a wind extreme occurs at this grid point on the same day, the day before, or the day after. We have further tested a regression model that includes a time lagged predictor variable to account for potential autocorrelation of the extreme precipitation, and the results are virtually identical. See *Mahlstein et al.* [2012] for more information on the lagged predictor logistic regression model.

5. Results

5.1. Global Quantification of Cooccurring Extremes

The percentage of concomitant precipitation and wind extremes, i.e., events happening on the same day or shifted by 1 day, at every grid point in DJF and JJA is shown in Figure 1. For comparison, counts of concomitant extremes happening on the same day are shown in the supporting information (Figure S4). In DJF high percentages of concomitant extremes are found along the west coasts of North America, Europe, and southern South America. Further areas with high percentages are the east coast of Greenland, the east coast of Asia (north of approximately 40°N), almost the entire coast of Antarctica, and tropical cyclone areas in the Southern Hemisphere, such as the western Indian Ocean and along the coast of Australia (Figure 1a). In these hot spot regions, the percentage values range between 30% and more than 50% of concomitant extremes.

During JJA high percentages of concomitant extremes are found in the tropical cyclone hot spots of the Northern Hemisphere (e.g., Caribbean, South China Sea, and Bay of Bengal) and also over Southeast Asia and along the west coasts of Canada and Alaska, southern south America, Australia, and New Zealand. Further on high percentages of concomitant extremes are found along the coast of Greenland and along almost the entire coastline of Antarctica.

The results of the logistic regression agree very well with the count-based analysis (Figures 2a and 2b). Regions with high percentages of concomitant events also show increased odds of joint extremes. The logistic regression analysis extends the count-based analysis by indicating statistically significant links between wind and precipitation extremes. In addition, the results show that there are also areas where the odds for a precipitation extreme to occur, given that extreme winds prevail, are reduced (Figures 2a and 2b). These areas with odds ratios smaller than 1 are found mainly in the tropics and over mountainous areas and are all not statistically significant.

5.2. Sensitivity to the Spatial Window

Compound extremes can be associated with the same weather system but occur in slightly different locations. This is often the case in extratropical cyclones [*Bengtsson et al.*, 2009]. The requirement that extremes need to occur at the same grid point is hence quite restrictive, and the results discussed so far are an indication of the lower limit of the number of concomitant wind and precipitation extremes. Therefore, the sensitivity to relaxing the definition of concomitant extremes is tested next. We allow a 1° spatial shift of

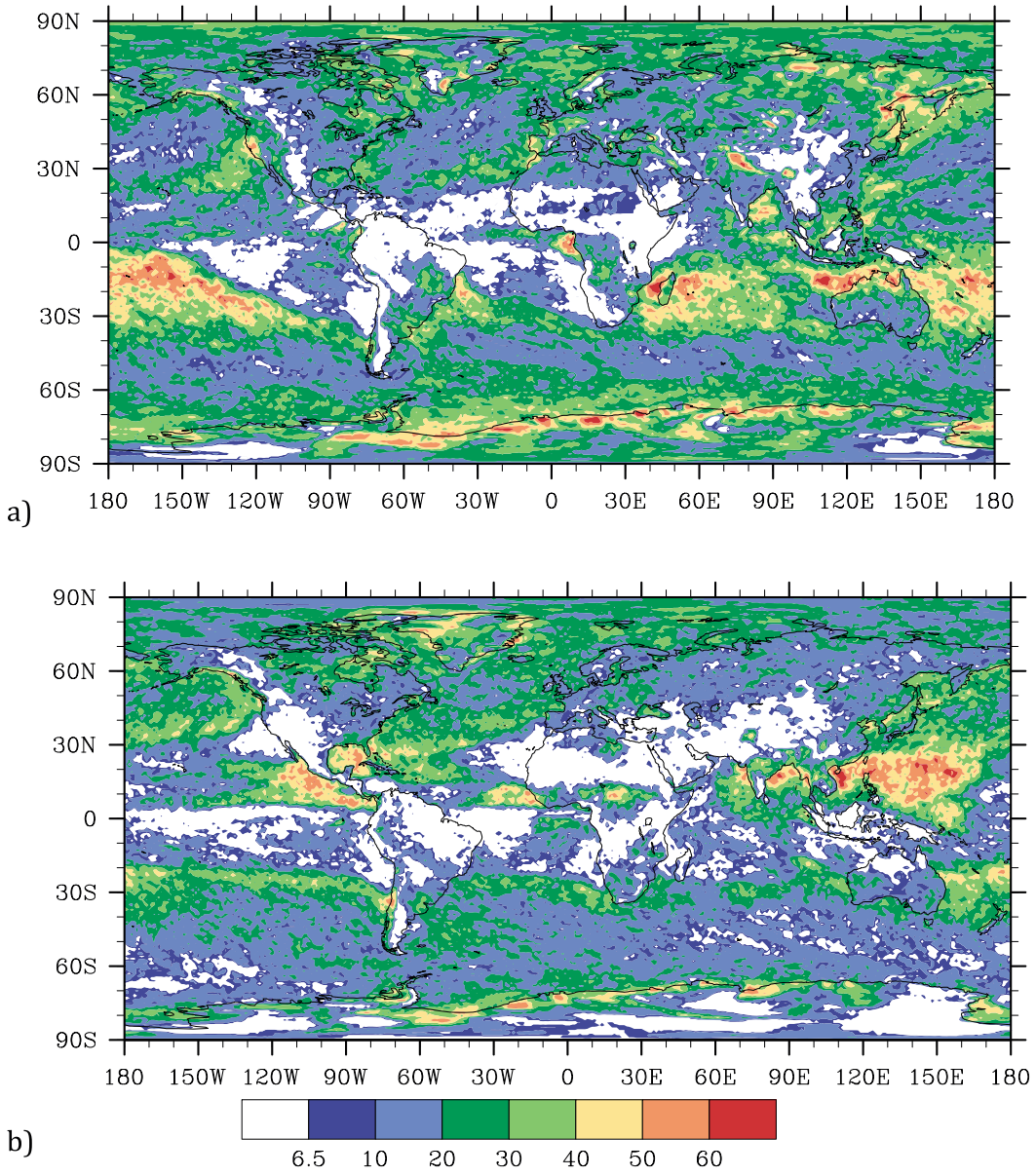

Figure 1. Percentage (%) of concomitant extremes taking 1 day shifts into account relative to all extremes from 1979 to 2012 during (a) DJF and (b) JJA.

the extremes (but no temporal shift) by considering precipitation extremes occurring at the eight grid cells next to the grid cell with the wind extreme as well (Figure 3).

Along the west coast of Europe but also in the Mediterranean area, more than 50% of the extremes occur concomitantly in DJF, if neighboring grid points are taken into account (Figure 3). The increase due to taking into account neighboring grid points is quite uniform in space in most areas of the globe and varies between 10% and 15%. Exceptions are the areas where the percentage of joint extremes is very low, for example, in the tropical Atlantic (Figure 4c).

If we look at domain average effects for Europe (20°N to 80°N and 10°W to 50°E), we find approximately 18% of concomitant extremes located at the same grid point. If a spatial shift of 1° is allowed, the percentage increases to 26%. The increase is strongest in relative terms in areas with low initial counts of concurrent extremes. Note that the large areas with low absolute percentages dominate the domain mean values.

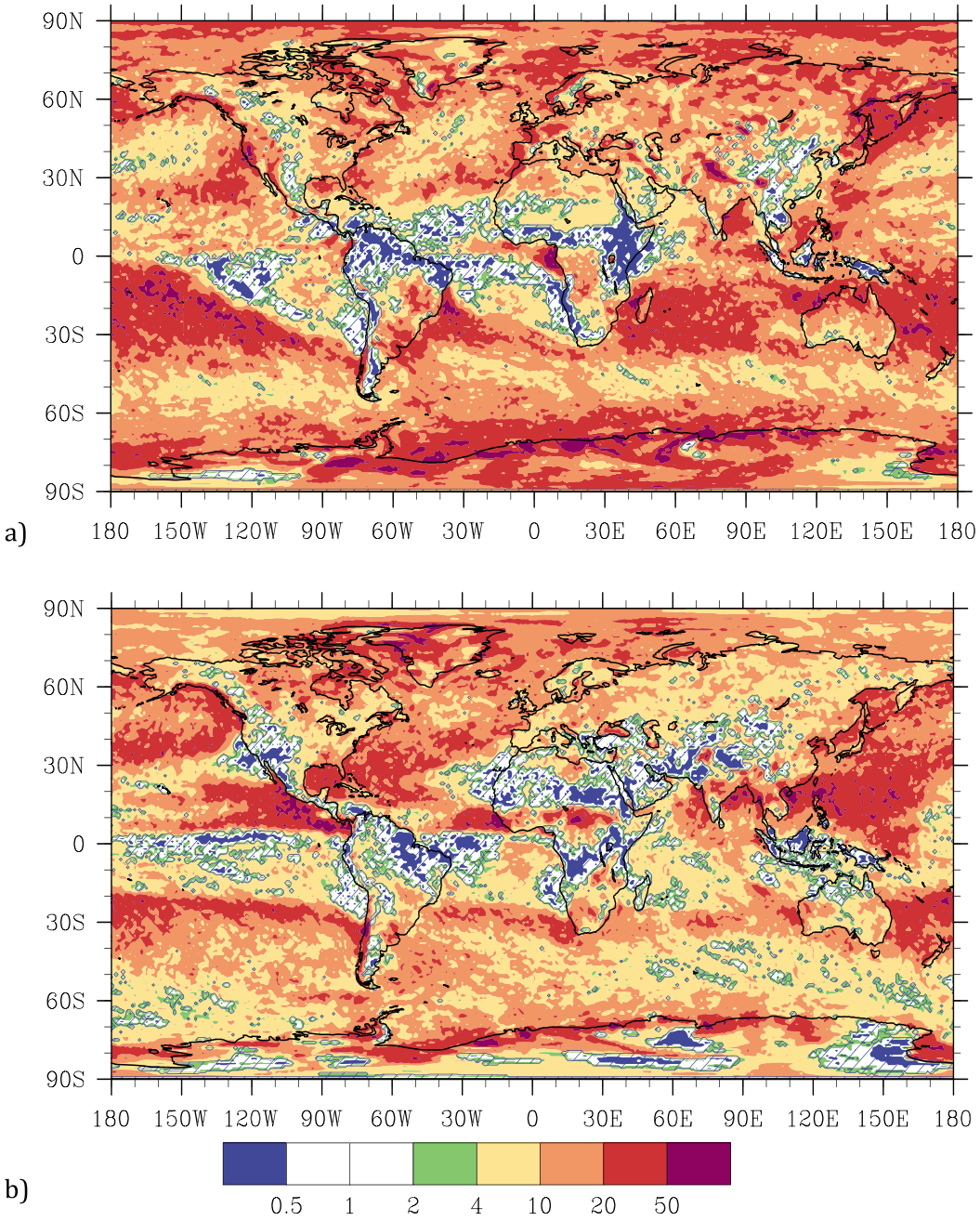

Figure 2. Odds ratio ($\exp(\beta_1)$) shaded, statistically nonsignificant areas are hatched in blue for (a) DJF and (b) JJA.

Hence, a relaxation of the matching criteria affects the absolute numbers. The motivation for the extension of the spatial matching criterion stems from insurance applications, where all losses associated with the same weather system are treated as one event and aggregated. Here we choose a simple spatial extension by one grid point in all directions for a sensitivity test. For insurance applications the correct way of doing this would be to take into consideration all areas that are affected by the same weather system [see, e.g., *Leckebusch et al.*, 2008; *Nissen et al.*, 2010].

5.3. Meteorological Processes Leading to Cooccurring Extremes

We now discuss the meteorological processes associated with cooccurring precipitation and wind extremes, focusing primarily on Europe during DJF. Figures 4a and 4b show the percentage of concomitant extremes

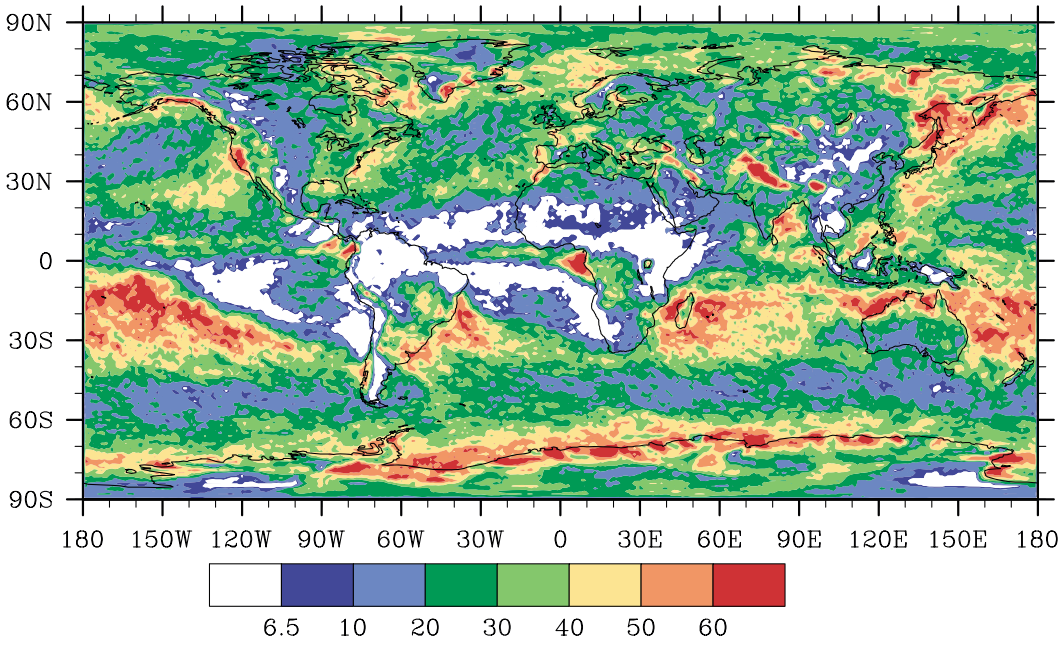

Figure 3. Percentage (%) of concomitant extremes in DJF counting extremes on the same day occurring at the same or the surrounding grid points.

and odds ratios in DJF as in Figures 1a and 2a, respectively, but for a domain over Europe (20°N to 80°N and 10°W to 50°E). The highest percentages and the highest odds ratios are found over the North and Baltic Seas, along the west coast of Spain, over northwestern central Europe, along the west coast of Norway, and over Israel and Syria. Areas with small and partially nonsignificant odds ratios are located over eastern Norway and Sweden, eastern Spain, Scotland, eastern central Europe, and North Africa (Figure 4b). These spatial patterns can be explained partly by orographic effects and partly by the characteristics of the weather systems that lead to extremes in specific areas.

In DJF wind and precipitation extremes in the midlatitudes and subtropics are often related to cyclones [*Pfahl*, 2014; *Raveh-Rubin and Wernli*, 2015; *Seneviratne et al*., 2012]. Regional variations in the cooccurrence of the extremes are due to differences in the relative positioning of the cyclone centers and the extremes. For instance, both extreme wind and precipitation events in the region northwest of the Alps are typically associated with cyclones over the North Sea [*Pfahl*, 2014], such that the same low-pressure system can induce both types of weather extremes in this region. This is in agreement with the high count of concurrent extremes in this area (Figure 4a). On the contrary, extreme precipitation east of the Alps is linked to Mediterranean cyclones that bring moist air into the area, whereas wind extremes are caused by cyclones passing over northern Europe [*Pfahl*, 2014]. Hence, different weather systems are responsible for wind and precipitation extremes and as a consequence the number of concurrent extremes is lower (Figure 4a).

Furthermore, topographic effects cause regional variations in the odds ratios. For example, the low odds ratios in the lee of mountains oriented perpendicular to the prevailing flow (eastern Norway, eastern Spain, eastern Scotland, and also central North America and eastern South America; see Figures 1 and 2) are likely linked to an orographic enhancement of rain on the windward side of the mountain chains and hence a drying of the air by the time it reaches the lee of the mountains. In some cases, Föhn effects with strong precipitation occurring on the windward side and very strong downslope winds in the lee of the mountains might additionally contribute to very small odds ratios. Two example cases of strong European windstorms, illustrating the drying effects by orography, are shown in Figures 4c and 4d. Windstorm Dagmar affected Scandinavia on 26 December 2011, and windstorm Xynthia affected Spain and France on 27 February 2010 (see *Liberato et al*. [2013] for a description of the impacts). In both cases, heavy precipitation occurred only on the windward side of the mountains, while the extreme winds extended much farther eastward (Figures 4c and 4d).

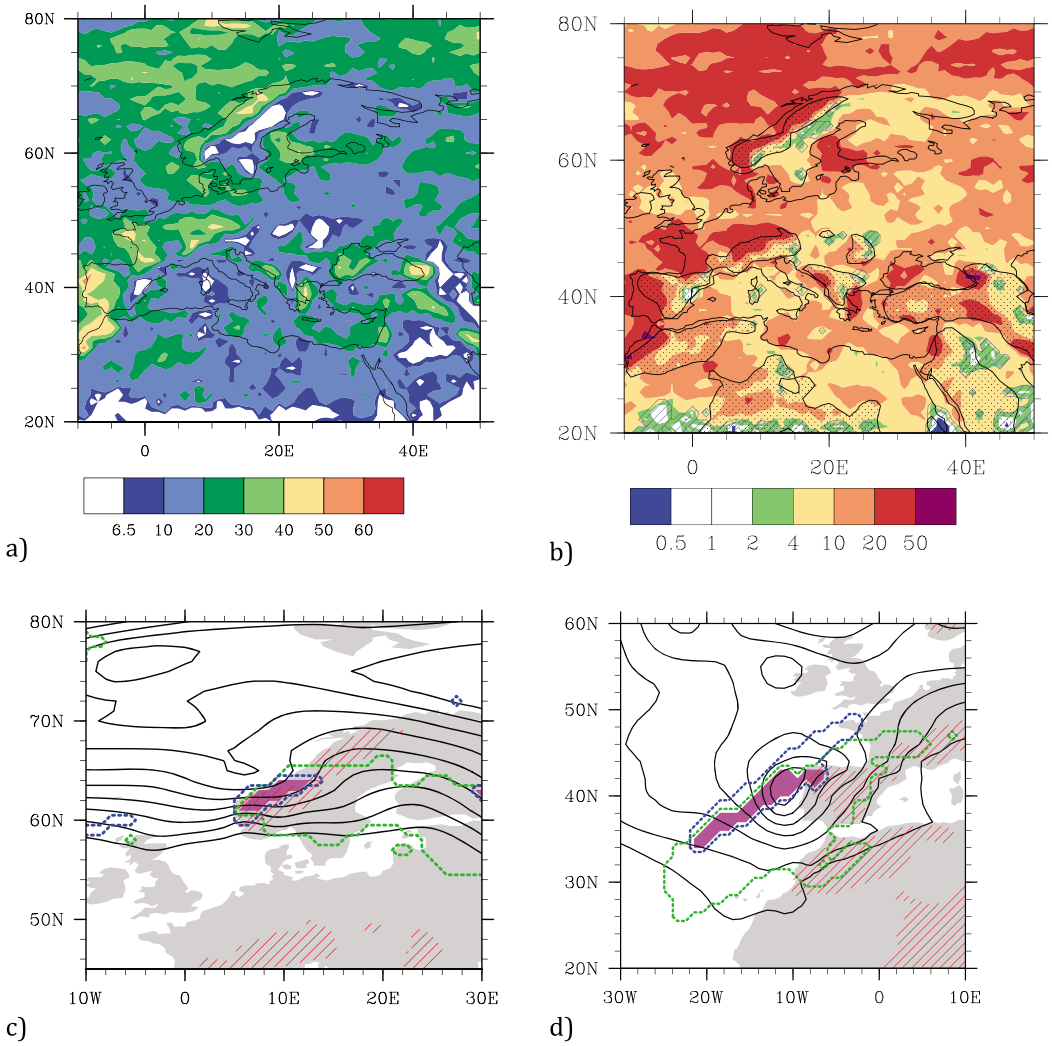

Figure 4. (a) Same as Figure 1a but zoomed on Europe; (b) same as Figure 2a but zoomed on Europe. The dotted areas highlight ERA-Interim topography exceeding 500 m asl (above sea level). (c) Winter storm Dagmar on 26 December 2011. The thick black lines indicate the sea level pressure at 18 UTC (970 hPa to 1010 hPa in steps of 5 hPa), blue dashed lines indicate areas with extreme precipitation, green lines indicate areas with extreme winds, and the magenta area the simultaneous extremes, red stippling highlights ERA-Interim topography exceeding 500 m asl. (d) Same as Figure 4c but shown is storm Xynthia on 27 February 2010, the sea level pressure field is shown at 12 UTC (980 hPa to 1010 hPa in steps of 5 hPa).

In other areas, local intense and dry wind systems tied to specific orographic settings and large-scale weather conditions explain some of the strong regional variations in the odds ratios. For example, the low odds ratios north and south of the Pyrenees (Figure 4b) might be linked to Tramontana and Cierzo winds [see, e.g., *Georgelin and Richard*, 1996; *Tout and Kemp*, 1985]. Other examples are the areas along the west coast of Central America with very low odds ratios in DJF (Figure 2a). In these areas the strong and dry Tehuantepecer gap winds [e.g., *Schultz et al.*, 1997] occur several times every winter.

6. Limitations of the Data Set and the Methodology

Large areas with nonsignificant odds ratios and sometimes odds ratios smaller than 1 are located in the subtropics, e.g., over subtropical Africa and in some Monsoon areas. These results should be interpreted with care for the following two reasons: (i) In these areas there is limited trust in the quality of the extreme precipitation data [see *Pfahl and Wernli*, 2012]. (ii) The subtropics are subject to a strong seasonal cycle in

precipitation extremes (Figure S2), and precipitation "extremes" in the dry season correspond to very low absolute values of the 98th percentiles (Figure S2).

The quality of the precipitation and wind data is limited by the relatively coarse resolution of the ERA-Interim data set (approximately 100 km grid spacing). Compared to working with high-resolution station data, the coarse resolution data set has the advantage that a spatial aggregation of the data is not necessary. However, an explicit representation of potentially important processes related to concomitant precipitation and wind extremes, such as small-scale convective processes, is missing. In addition, convection associated with large-scale forcing, which was shown to be important for winter storm Kyrill [*Fink et al*., 2009] and is relevant for sting jet cases [*Gray et al*., 2011], might also not be fully represented in the data set.

Finally, the results presented here are tightly coupled to the definition of the extremes, here the local seasonal 98th percentile, and they do not necessarily apply also to very rare extremes. To analyze the cooccurrence of or the dependence between very rare extremes, different statistical methods should be used [*Coles et al*., 1999].

7. Conclusions and Outlook

Compound wind and precipitation extremes, i.e., the concomitant occurrence of extreme winds and precipitation, are investigated using ERA-Interim daily precipitation and wind gust data from January 1979 to December 2012. Extremes are defined as exceedances of the local seasonal 98th percentile. This corresponds to "moderate" extremes that can be impact relevant.

Areas with statistically significant cooccurrence of precipitation and wind extremes are found around the globe. In some densely populated and potentially high-impact areas in western Europe, along the west coast of North America and the west coast of South America, the percentage of concomitant extremes reaches up to more than 45%, even with a very conservative approach, considering only extremes that occurred on the same day or the previous or following day and at the same grid point. The percentage increases to more than 50% if the cooccurrence criterion is relaxed, and events that are shifted by one grid point (approximately 100 km) are counted as well. There are good arguments in favor of the spatial relaxation based on the typical size, structure, and life cycle of extratropical and tropical cyclones [e.g., *Bengtsson et al*., 2009]. An extension of the temporal shift to more than 1 day is conceivable, if good arguments from an impact perspective exist, i.e., if severe impacts can be expected even if the extreme events are separated by more than 1 day.

The number of concomitant extremes varies substantially with the season and in space. Very strong regional gradients in the number of concomitant extremes exist, which are linked to distinct local flow processes. In the extratropics, these variations can be explained partly by orographic effects and partly by the characteristics of the weather systems (cyclones) associated with the extremes. The spatial structure of the joint occurrence of wind and precipitation extremes and link to topography and weather systems has been discussed in some detail for Europe. It is possible to extend some of these findings to other regions around the world, e.g., the orographic and Föhn (Chinook) effects; there are, however, many other interesting spatial patterns, especially in the subtropics and tropics, whose detailed discussion is beyond the scope of this paper.

The methodology is simple and computationally fast and could easily be applied to analyze the frequency of and changes in compound "moderate" extremes in gridded data sets such as the Coupled Model Intercomparison Project Phase 5 (CMIP5) or the Coordinated Regional Climate Downscaling Experiment (Cordex) data sets.

Acknowledgments
The ERA-Interim reanalysis data set is available from the European Centre for Medium Range Weather forecasts http://www.ecmwf.int/en/research/climate-reanalysis/era-interim. The R code is available from the authors upon request. We thank Joaquim Pinto and one anonymous reviewer for valuable feedback that led to an improvement of the clarity and content of the paper.

References

Bengtsson, L., K. I. Hodges, and N. Keenlyside (2009), Will extratropical storms intensify in a warmer climate?, *J. Clim.*, *22*, 2276–2301, doi:10.1175/2008JCLI2678.1.

Coles, S., J. Heffernan, and J. Tawn (1999), Dependence measures for extreme value analyses, *Extremes*, *2*, 339–365.

Dee, D. P., et al. (2011), The ERA-Interim reanalysis: Configuration and performance of the data assimilation system, *Q. J. R. Meteorol. Soc.*, *137*, 553–597.

Federal Emergency Management Agency (2013), Multi-hazard loss estimation methodology: Hurricane model Hazus®–MH MR5, Tech. Manual, Dep. of Homeland Security Federal Emergency Manage, Agency Mitigation Div., Washington, D. C.

Fink, A. H., T. Brucher, V. Ermert, A. Kruger, and J. G. Pinto (2009), The European storm Kyrill in January 2007: Synoptic evolution, meteorological impacts and some considerations with respect to climate change, *Nat. Hazard Earth Syst. Sci*, *9*, 405–423.

Froidevaux, P., J. Schwanbeck, R. Weingartner, C. Chevalier, and O. Martius (2015), Flood triggering in Switzerland: The role of daily to monthly preceding precipitation, *Hydrol. Earth Syst. Sci.*, *19*, 3903–3924, doi:10.5194/hess-19-3903-2015.

Georgelin, M., and E. Richard (1996), Numerical simulation of flow diversion around the Pyrenees: A tramontana case study, *Mon. Weather Rev.*, *124*, 687–700, doi:10.1175/1520-0493(1996)124.

Gray, S. L., O. Martinez-Alvarado, L. H. Baker, and P. A. Clark (2011), Conditional symmetric instability in sting-jet storms, *Q. J. R. Meteorol. Soc.*, *137*, 1482–1500, doi:10.1002/qj.859.

Guzzetti, F., S. Peruccacci, M. Rossi, and C. P. Stark (2008), The rainfall intensity-duration control of shallow landslides and debris flows: An update, *Landslides*, *5*(1), 3–17, doi:10.1007/s10346-007-0112-1.

Kew, S. F., F. M. Selten, G. Lenderink, and W. Hazeleger (2013), The simultaneous occurrence of surge and discharge extremes for the Rhine delta, *Nat. Hazard Earth Syst. Sci*, *13*, 2017–2029, doi:10.5194/nhess-13-2017-2013.

Klawa, M., and U. Ulbrich (2003), A model for the estimation of storm losses and the identification of severe winter storms in Germany, *Nat. Hazard Earth Syst. Sci*, *3*, 725–732.

Leckebusch, G. C., D. Renggli, and U. Ulbrich (2008), Development and application of an objective storm severity measure for the Northeast Atlantic region, *Meteorol. Z.*, *17*, 575–587, doi:10.1127/0941-2948/2008/0323.

Liberato, M. L. R. (2014), The 19 January 2013 windstorm over the North Atlantic: Large-scale dynamics and impacts on Iberia, *Weather Clim. Extremes*, *5–6*, 16–28, doi:10.1016/j.wace.2014.06.002.

Liberato, M. L. R., J. G. Pinto, P. Ludwig, P. Ordonez, D. Yuen, and I. F. Trigo (2013), Explosive development of winter storm Xynthia over the subtropical North Atlantic Ocean, *Nat. Hazard Earth Syst. Sci.*, *13*, 2239–2251, doi:10.5194/nhess-13-2239-2013.

Mahlstein, I., O. Martius, C. Chevalier, and D. Ginsbourger (2012), Changes in the odds of extreme events in the Atlantic basin depending on the position of the extratropical jet, *Geophys. Res. Lett.*, *39*, L22805, doi:10.1029/2012GL053993.

Nissen, K. M., G. C. Leckebusch, J. G. Pinto, D. Renggli, S. Ulbrich, and U. Ulbrich (2010), Cyclones causing wind storms in the Mediterranean: Characteristics, trends and links to large-scale patterns, *Nat. Hazard Earth Syst. Sci.*, *10*, 1379–1391, doi:10.5194/nhess-10-1379-2010.

Pfahl, S. (2014), Characterising the relationship between weather extremes in Europe and synoptic circulation features, *Nat. Hazard Earth Syst. Sci*, *14*, 1461–1475, doi:10.5194/nhess-14-1461-2014.

Pfahl, S., and H. Wernli (2012), Quantifying the relevance of cyclones for precipitation extremes, *J. Clim.*, *25*, 6770–6780, doi:10.1175/JCLI-D-11-00705.1.

Raveh-Rubin, S., and H. Wernli (2015), Large-scale wind and precipitation extremes in the Mediterranean: A climatological analysis for \1979–2012, *Q. J. R. Meteorol. Soc.*, *141*, 2404–2417, doi:10.1002/qj.2531.

Rodgers, E. B., S. W. Chang, and H. F. Pierce (1994), A satellite observational and numerical study of precipitation characteristics in western North-Atlantic tropical cyclones, *J. Appl. Meteorol.*, *33*, 129–139, doi:10.1175/1520-0450(1994)033<0129:Asoans>2.0.Co;2.

Schultz, D. M., W. E. Bracken, L. F. Bosart, G. J. Hakim, M. A. Bedrick, M. J. Dickinson, and K. R. Tyle (1997), The 1993 superstorm cold surge: Frontal structure, gap flow, and tropical impact, *Mon. Weather Rev.*, *125*, 662–662.

Seneviratne, S. I., et al. (2012), Changes in climate extremes and their impacts on the natural physical environment, in *Managing the Risks of Extreme Events and Disasters to Advance Climate Change Adaptation*, *A Special Report of Working Groups I and II of the Intergovernmental Panel on Climate Change (IPCC)*, edited by C. B. Field et al., pp. 109–230, Cambridge Univ. Press, U. K., and New York.

Tout, D. G., and V. Kemp (1985), The named winds of Spain, *Weather*, *40*, 322–329, doi:10.1002/j.1477-8696.1985.tb03721.x.

Witte, J. C., A. R. Douglass, A. da Silva, O. Torres, R. Levy, and B. N. Duncan (2011), NASA A-Train and Terra observations of the 2010 Russian wildfires, *Atmos. Chem. Phys.*, *11*, 9287–9301, doi:10.5194/acp-11-9287-2011.

Zhang, X. B., L. Alexander, G. C. Hegerl, P. Jones, A. K. Tank, T. C. Peterson, B. Trewin, and F. W. Zwiers (2011), Indices for monitoring changes in extremes based on daily temperature and precipitation data, *Wires Clim. Change*, *2*, 851–870.